COBEM 99
XV Congresso Brasileiro de Engenharia Mecânica
15th Brazilian Congress of Mechanical Engineering
22 - 26 de Novembro de 1999 / November 22 - 26, 1999 Águas de Lindóia, São Paulo,

PARTICLE IMAGE VELOCIMETRY MEASUREMENTS AT THE ENTRANCE REGION OF A ONE-SIDED HEATED VERTICAL CHANNEL IN NATURAL CONVECTION

L. F. A. Azevedo
B. A. A. Gomes
Departamento de Engenharia Mecânica, PUC-RIO
22453-900, Rio de Janeiro RJ, Brasil

Abstract. *The Particle Image Velocimetry Technique was employed to measure velocity fields at the entrance region of a one-sided heated vertical channel in natural convection. The experiments were aimed at revealing the extent of the region of influence of the channel on the entrance flow field, and to provide information on the shape of the velocity profile at the channel entrance plane. Three operating conditions of the channel were investigated corresponding to three values of the channel Rayleigh number. The results obtained revealed that the influence of the channel does not extend to a large region at the entrance of the channel. The velocity profile at the entrance was shown to have a significant horizontal component.*

Key-words: *Channel Flow, Natural Convection, Velocity Measurements*

1. INTRODUCTION

One-sided heated vertical channels in natural convection encounter applications in several industrial fields, ranging from the thermal control of ambients and electronic components, to the passive cooling of nuclear reactors. For that reason, this configuration has been extensively studied in the literature both experimentally and numerically (e.g. Elenbaas, 1942, Bar-Cohen and Rosenow, 1984).

In the literature available, no experimental information is found regarding the flow field characteristics of this natural convection configuration. The information available on the flow field is based on numerical solutions of the equations of conservation of mass, linear momemtun and energy. In these solutions, the computational domain is either limited to the channel region, as in the works of Bodoia and Osterle, 1962, Nieckele and Azevedo, 1987 and El-Shaarawi and Mokheimer, 1999, or is extended to a region far from the channel entrance, as in Kettleborough, 1972. In the first approach, the form of the velocity profile at the entrance of the channel is assumed. Flat velocity profiles or parabolic profiles have been used. In the second approach, the extent of the region upstream of the channel is chosen such that the fluid acceleration can be neglected at the boundary of the computation domain.

The objective of the present paper is to provide experimental information on the

velocity field in the vicinity of the channel entrance. This information can be used to aid the choice of the appropriate boundary conditions for numerical solutions.

A whole field velocimetry technique was implemented to measure the velocity fields at the channel entrance. The technique, known as Particle Image Velocimetry, is based on the analysis of consecutive images of tracer particles illuminated by a laser light sheet. As will be demonstrated, this technique provides a detailed view of the flow field at the entrance of the one-sided heated channel.

2. EXPERIMENTAL APPARATUS

2.1 Test section

The test section utilized in the experiments is described schematically in Figure 1. The main part of the test section was a 10-mm-thick copper plate with dimensions 180 x 120 mm (height x width), designed to deliver heat to the fluid isothermally. To this end, three independently controlled heaters were installed at the back surface of the plate. The heaters were constructed with 0.254-mm diameter, teflon-coated chromel wire and were powered by three variable transformers.

Temperature uniformity at the heating surface was obtained by adjusting the power to the three heaters. Eight, 0.127-mm-diameter, chromel-constantan thermocouples were installed in holes drilled through the back surface of the plate at 0.5 mm from the heating surface. These thermocouples distributed along the copper plate guided the adjusting process. A HP-3546 digital voltmeter was used for the thermocouples voltage readings. The heat losses from the heated plate to the ambient fluid were minimized by backing the copper plate with a 50-mm-thick styrene block.

A 6-mm-thick Plexiglass plate formed the unheated wall. The channel geometry was completed by two Plexiglass side walls attached to the principal walls. The heated copper plate, together with the unheated wall and the two side walls were mounted on a Plexiglass frame (not shown in the figure) designed so as not to obstruct the flow in and out of the channel. The Plexiglass walls allowed visual access to the interior of the channel, a necessary

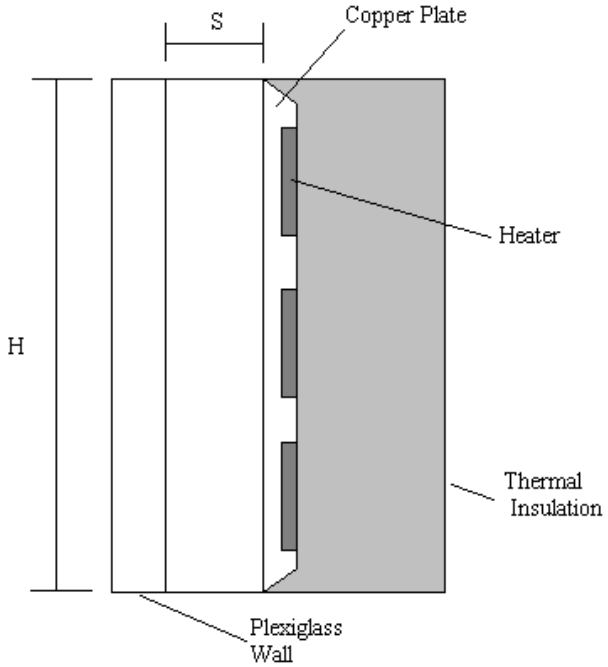

Figure 1 – Schematic view of the test section.

condition for the utilization of the optical velocity measurement technique employed.

The test section described above, was placed in a water-filled, glass tank with dimensions 400 x 400 x 500 mm (length x width x height). The tank was covered to avoid water losses due to evaporation. Three chromel-constantan (0.127-mm diameter) thermocoupless were vertically deployed in the tank. The thermocouples were mounted on a vertical support positioned, respectively, at 50, 200 and 400 mm from the tank floor. The readings of these thermocouples were used to determine the mean water temperature and to detect any undesirable temperature stratification.

2.2 Velocity measurements

Fluid flow velocity measurements were accomplished by the use of the Particle Image Velocimetry technique, PIV. This is an optical technique capable of performing instantaneous velocity measurements over extensive areas of the flow field. The technique is based on the analysis of consecutive images of tracer particles dispersed in the fluid and illuminated externally by a plane of light. By this method, depending on the particle concentration, several thousand velocity vectors can be measured simultaneously.

Figure 2 shows a schematic view of the velocity measurement system employed. Light from a 5-Watt laser, model Innova 70 by Coherent, is modulated by a Pockels cell, model 3455 manufactured by Connoptics. The beam exiting the Pockels cell is transformed into a diverging light sheet by a cylindrical lens. A spherical lens is also employed to control the thickness of the light sheet. The light sheet reaches the test section, after passing through the tank glass wall, illuminating the region of interest in the flow. The water in the tank was seeded with 20 μm, spherical, poliethylene particles. The particles have density of 1.05 g/cm^3, what guarantees that they faithfully follow the flow.

The images of the particles in the flow were registered by a TSI 60040 CCD cross correlation camera, mounted orthogonally to the illuminating light sheet. The camera has a spatial resolution of 640 x 480 pixels and a fixed frame rate of 30 frames per second. The camera was equipped with a 18-108 mm zoom lens. The images were digitized by a TSI model 6157 frame grabber, running on a Pentium 150 Mhz computer.

The synchronization of the camera with the laser modulation by the Pockels cell and the frame grabber, was performed by a TSI model 60030 synchronizer. The synchronizer locked to the start-of-frame camera signal and waited for a pre set time delay to activate the Pockels cell, producing the first illuminating pulse. After a specified time interval, the synchronizer triggered the Pockels cell again, producing the second illuminating pulse. In this way, the first light pulse was registered in one camera frame, while the second one was registered in the subsequent frame, with a time interval different from the fixed 33 ms interval characteristic of the camera. This technique, known as frame straddling, allows that images with relatively

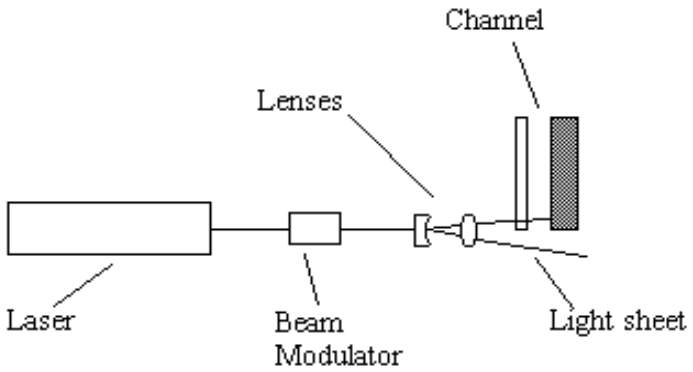

Figure 2 – Schematic view of the velocity measurement optical setup.

small time intervals be registered using cameras with standard frame rates. For instance, in the case of the camera used in the present experiments, intervals between images as low as 30 μs can be registered in a 30 frames per second camera.

The duration of each light pulse and the time between pulses can be set in the synchronizer. The time between pulses is the single most important parameter that determines the success of the measuring technique, and depends on the magnitude of the flow velocity being measured. Faster flows require smaller times between pulses to guarantee that the images of the particles registered in the second frame have not displaced too far from their positions in the first frame. If this is not the case, the correlation between the two images will fail to produce the desired particle displacements.

The larger the duration of the illuminating pulse, the brighter is the particle images and the easier is to register them in the camera. The duration of the pulses is limited by the particle velocity. Faster particles require small pulse duration, to avoid particle streaking.

Image Analysis. The velocity field was determined by cross correlating the two images of the particles corresponding to the two consecutive light pulses. Cross correlation is a very effective and robust technique of analyzing images with high density of particles, yielding particle displacement fields without directional ambiguity. A brief description of the cross correlation method is presented next. Further details of cross correlation as applied to PIV images can be found in several references (e.g., Adrian, 1996 and Almeida, 1997).

Figure 3(a) and (b) represent typical particle images captured at two consecutive time instants, t (image 1) and t + Δt (image 2). A window is selected in image 1 containing, at its center, the point where the velocity will be determined. The dimensions of this window, called the base window, are such that a reasonable number of particle images is contained in the window area. Typically, 10-20 particles produce good results (Adrian, 1996). If the window area is sufficiently small that velocity gradients are not strong, it is highly probable that the same pattern of particles in window 1 will be found somewhere in image 2. To find the location of the pattern of window 1 in image 2, a new window is selected in image 2. This window, the search window, is centered at the same coordinates of the point of measurement, but in image 2, and is used to limit the search area in image 2.

In Figure 4, $I_1(j,k)$ and $I_2(j,k)$ are the two windows, and (j,k) are indexes of the JxK pixels base window, positioned in the MxN pixels search window. The coordinates of the point where the measurement is being performed are (x_1,y_1).

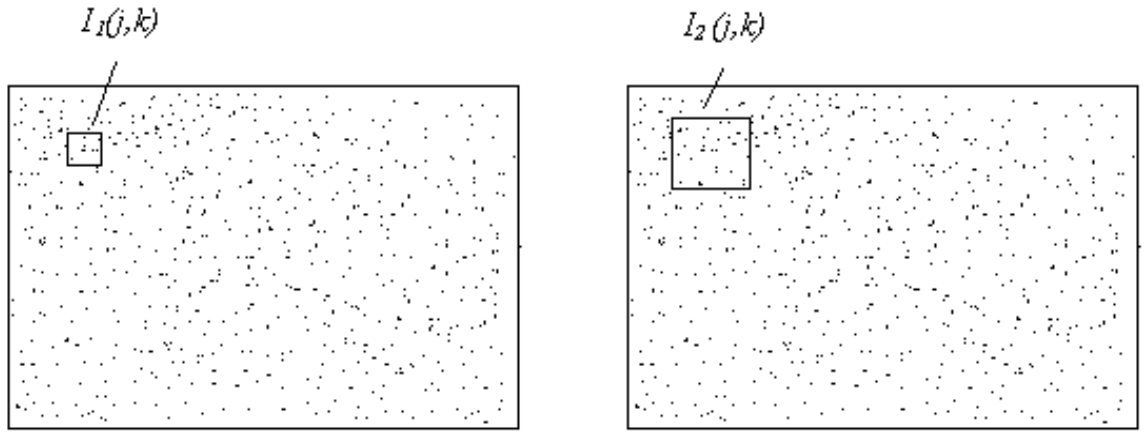

Figure 3 – Typical high particle concentration images.

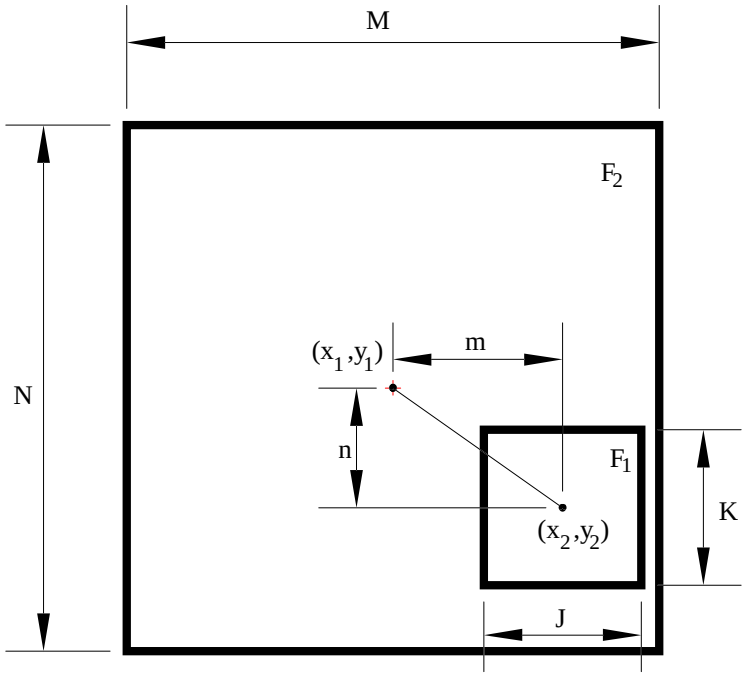

Figure 4 – The base and search windows for cross correlation analysis of the particle images.

By cross correlating the two windows, the pattern of window 1 is overlaid on window 2, with a pixel offset corresponding to the displacement being checked. The cross correlation function is the sum of the products of the aligned pixel values, and is given, in a normalized form, as (Almeida, 1997),

$$R(m,n) = \frac{\sum_j \sum_k I_1(j,k)\, I_2(j-m,k-n)}{\left\{\left[\sum_j \sum_k I_1^2(j,k)\right]\left[\sum_j \sum_k I_2^2(j-m,k-n)\right]\right\}^{1/2}} \qquad (1)$$

The position in window 2 where the correlation function R displays its largest value has coordinates (x_2,y_2), and determines the location where window 1 is found in window 2. The velocity vector is given by

$$u = (x_2 - x_1)/ M\,\Delta t \quad e \quad v = (y_2 - y_1)/ M\,\Delta t \qquad (2)$$

where, M is the magnification of the image and Δt the time interval between the two images.

Since the correlation function is normalized, its values vary between zero and one. However, due to deformations imposed on the pattern of window 1 by the flow, or by the possibility of particles being lost out of window 2, the correlation value will be smaller than one. For this reason, it is necessary to impose a threshold value bellow which the correlation is not considered valid.

A typical map of the correlation function is presented in Figure 5. The coordinates of the base region are (x_1=0, y_1=0), and the coordinates (x_2,y_2) correspond to the point where the correlation is maximum, that is, the tallest peak in the correlation map.

The calculation of the cross correlation function by the convolution of the two image functions as presented in the previous paragraphs, is a computationally intensive task. A more

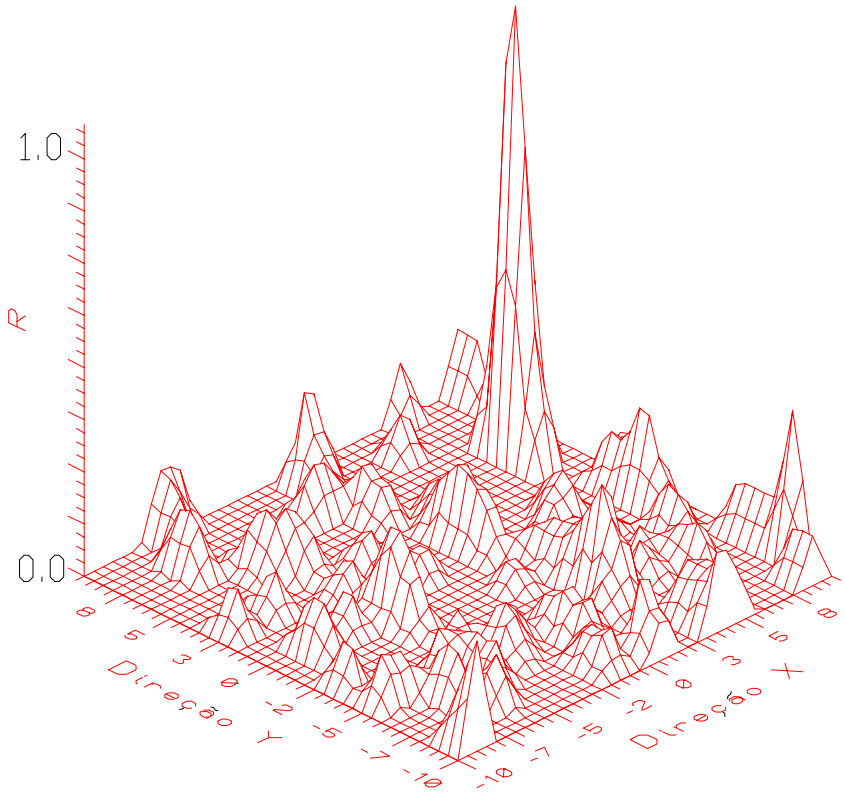

Figure 5 – Typical map of cross correlation function.

efficient alternative is to compute the cross correlation function using two dimensional Fast Fourier Transforms (FFT). In this method, the FFT of window 1 is multiplied by the complex conjugate of the FFT of window 2. The inverse FFT of the multiplication result is the correlation function. The results to be presented in this paper were obtained using this method, as implemented in the INSIGHT Particle Image Velocimetry software by TSI.

2.3 Data reduction

The velocity fields results will be presented in this paper in terms of the channel Raleigh number based on the inter-plate spacing, S. This dimensionless number is calculated as (Nieckele and Azevedo, 1987)

$$(S/H)Ra_S = (S/H)\left[g\beta\left(T_w - T_\infty\right) S^3/\nu^2\right]\Pr \tag{3}$$

where S is the inter-plate spacing, H is the channel height, g the acceleration of gravity, β is the coefficient of thermal expansion, ν the fluid kinematic viscosity and Pr the fluid Prandtl number. The wall temperature, T_w, was calculated by averaging the readings of the eight plate thermocouples. The fluid ambient temperature, T_∞, was also calculated by averaging the readings of the three thermocouples placed in the test tank. All the fluid properties were evaluated at the film temperature $T_f = (T_w+T_\infty)/2$.

3. RESULTS AND DISCUSSION

As mentioned in the Introduction, the objective of the present work is to furnish information regarding the velocity field at the entrance of the one-sided heated vertical channel configuration. To this end, the light sheet was positioned so as to illuminate the region adjacent to the channel entrance and the initial portion of the channel.

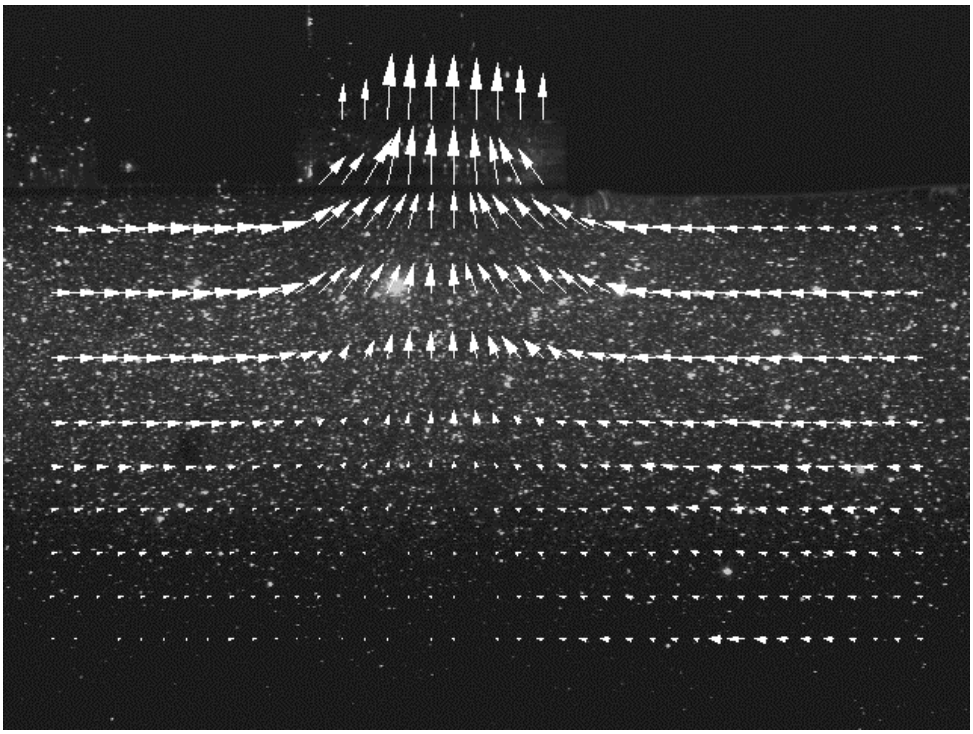

Figure 6 – Velocity field overlaid on particle image for $(S/H)Ra_S = 5.6 \times 10^4$ and Pr = 5.2.

Three values of the channel Rayleigh number investigated were selected for presentation: $(S/H)Ra_S = 6.7 \times 10^3$, 2.1×10^4 and 5.6×10^4. These values correspond to plate-to-ambient temperature differences of, respectively, 2, 6 and 13 ^oC, and an inter-plate spacing, S, of 14 mm.

Figure 6 presents the actual particles image with the measured velocity field overlaid on it, for $(S/H)Ra_S = 5.6 \times 10^4$ and Pr = 5.2. The particle image shown would correspond to image 1 in the description of the cross correlation technique presented before. The dark rectangular region at the top right of the figure is the lower part of the copper heating plate, together with its back insulation. The somewhat smaller, dark rectangular region to the left is the lower part of the unheated Plexiglass wall. The lower part of the channel is the lighter region between these two dark regions. The remaining of the channel extends upward, and it is not shown in the figure.

The two images of the particles were captured with a time interval of 33.4 ms. The laser power was set to 2.2 W, and the camera *f* number was set to 11. The images were cross correlated using a 32x32 pixel window. This window size proved to be adequate for the particular flow field and particle concentration level, since no invalid vectors were obtained in the whole flow field area searched (an invalid vector is the one in which the cross correlation function did not attain a value above the threshold value set). The 32x32 window correspond to a 2.5 x 2.5 mm area in the actual flow. This is the spatial resolution of the measurements performed. For each new velocity measurement, the window was displaced of 16 pixels in the horizontal and vertical directions. A total of 1200 vectors were measured from the images. Not all these vectors are displayed in Figure 6, so as not to over crowd the figure.

An inspection of the results presented in Figure 6 reveals the pattern of flow field driven by the natural convection flow. The fluid far from the channel entrance is nearly at rest, being accelerated smoothly toward the channel. One important information drawn from the results presented in Figure 6, is the extent of the region of influence of the channel. It can be seen that at a vertical distance of approximately two channel inter-plate spacings down from the entrance plane, the flow can be considered as having negligible acceleration. Also, in the horizontal direction, the fluid velocity at a distance of two inter-plate spacings has also

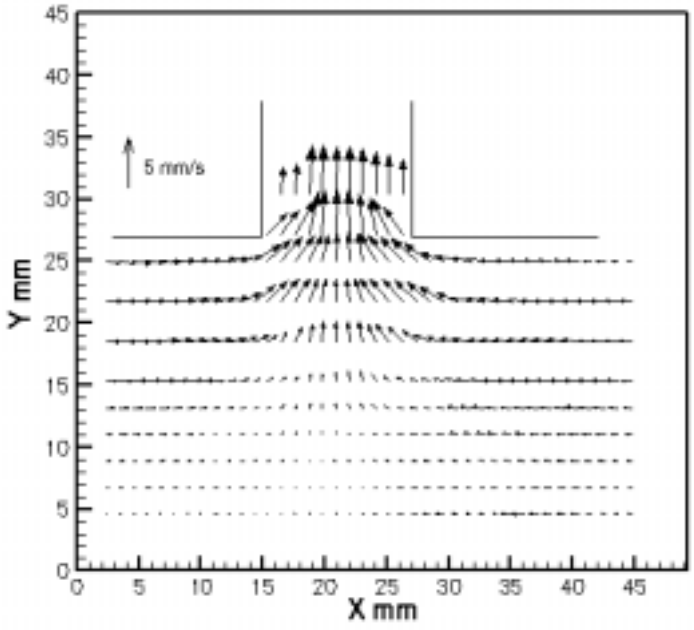

Figure 7 – Velocity field at channel entrance for $(S/H)Ra_S = 5.6 \times 10^4$ and Pr = 5.2.

negligible acceleration. This information can be useful for numerical solutions of the problem, where, as already mentioned in the Introduction, the knowledge of the region where the flow has zero acceleration determines the size of the computational domain to be employed in the calculations.

The cross-channel velocity profiles at the beginning of the channel are also shown in Figure 6. The rapid development flow process in the channel can be observed. Velocity measurements closer to the channel walls were not possible due to limitations in the camera spatial resolution, and should not be attributed to an intrinsic limitation of the technique employed.

The magnitude of the velocity vectors can be better assessed with the help of Figure 7. In this figure, the same velocity data presented in Figure 6 are plotted without the particle images. The channel entrance is schematically represented in the figure for reference purpose. The figure also displays a reference velocity vector.

An interesting observation can be made with regard to the velocity profile at the channel entrance plane. It can be verified that a significant horizontal velocity component is present at the channel entrance. Some numerical solutions of the natural convective flow through vertical channels have made use of a purely vertical velocity profile with zero horizontal component at the entrance (Bodoia and Osterle, 1962, Nieckele and Azevedo, 1987 and El-Shaarawi and Mokheimer, 1999).

Figures 8 and 9 present the velocity field measured at the channel entrance region respectively for $(S/H)Ra_S = 2.1 \times 10^4$ and 6.7×10^3 . In both cases the Prandtl number is equal to 5.9. In the figures only the measured velocity fields are presented, without the particles images. The parameters employed to capture and cross correlate each pair of images were the same as those described for Figure 6 and 7.

The overall features of the velocity field are similar to those described for the higher $(S/H)Ra_S$ case of Figure 6. However, the magnitude of the velocity vectors are smaller, as would be expected. Also, due to the smaller velocity levels, the regions of influence of the channel are reduced when compared to the higher channel Rayleigh number case of Figure 6 and 7.

4. CONCLUSIONS

The velocity field in the neighborhood of the entrance of a one sided-heated vertical channel in natural convection was investigated experimentally. The velocity fields were measured employing a whole field velocimetry technique based on cross correlation of successive image of small tracer particles distributed in the fluid.

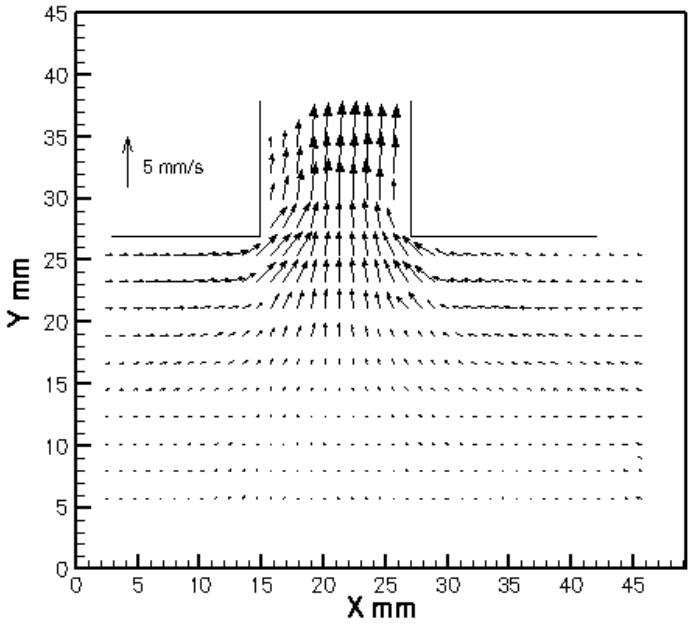

Figure 8 – Velocity field at channel entrance for $(S/H)Ra_S = 2.1 \times 10^4$ and Pr = 5.9.

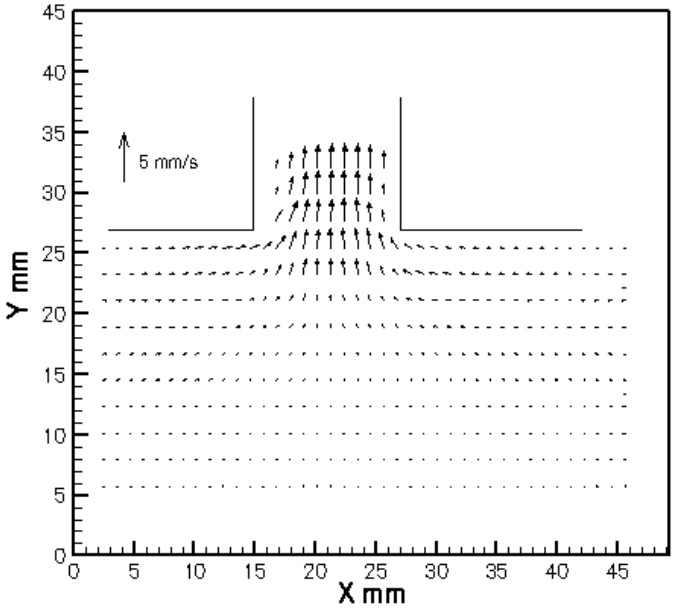

Figure 9 – Velocity field at channel entrance for $(S/H)Ra_S = 6.7 \times 10^3$ and Pr = 5.9.

The measurements have shown that the region of influence of the channel extends a distance equivalent to only a few inter-plate spacings from the channel entrance. Also, it was demonstrated that a significant horizontal component is present in the velocity profile at the channel entrance. The information obtained on the velocity field at the channel entrance region is useful to guide the choice of velocity boundary conditions for numerical simulations of the problem.

REFERENCES

Adrian, R.J., 1996, Laser Velocimetry, in Fluid Mechanics Measurements, ed. Goldstein, Taylor and Francis, Washington.

Almeida, J.A., 1997, Particle Image Velocimetry System, Doctoral Thesis, Department of Mechanical Engineering, *PUC-RIO,* in portuguese.

Bar-Cohen, A. and Rosenow, W.M., 1984, Thermally Optimum Spacing of Vertical, Natutal Convection Cooled, Parallel plates, J. Heat Transfer, vol. 106, pp. 116-123.

Bodoia, J.R. and Osterle, J.F., 1962, The Development of Free Convection Between Vertical Plates, ASME J. Heat Transfer, vol. 84, pp. 40-44.

Elenbaas, W., 1942, Heat Dissipation of Parallel Plates by Free Convection, Physica,vol. 9, pp. 1-28.

El-Shaarawi, M.A.I. and Mokheimer, E.M.A., 1999, Developing Free Convection in Open-Ended Vertical Eccentric Annuli With Isothermal Boundaries, ASME J. Heat Transfer, vol. 121, pp. 63-72.

Kettleborough, C.F., 1972, Transient Laminar Free Convection Between Heated Vertical Plates Including Entrance Effects, Int. J. Heat Mass Transfer, v. 15, pp. 883-896.

Nieckele, A.O. and Azevedo, L.F.A., 1987, Reverse Flow in One-Sided Heated Vertical Channels in Natural Convection, in Convective Transport HTD-82, ASME Winter Annual Meeting, Boston, Massachusetts, pp. 71-77.